Neurosci Bull December 1, 2009, 25(6): 376-382. http://www.neurosci.cn
DOI: 10.1007/s12264-009-0605-0

·Original Article·

Nasal cavity-maxillary sinus-pterygopalatine fossa-Meckel's cave: a preliminary anatomic study of an endoscopy-based operative approach

Zhi-Qiang BAI[1], En-Yuan CAI[1], Shi-Qiang WANG[1], Zhao-Jian LI[1], Shou-Biao WANG[2]

[1]*Department of Neurosurgery, Affiliated Hospital of Qingdao University Medical College, Qingdao 266003, China*
[2]*Department of Anatomical Sciences, Qingdao University Medical College, Qingdao 266071, China*

Abstract: Objective To provide a new approach for the treatment of tumor in Meckel's cave, by dissecting adjacent structures of the nasal cavity-maxillary sinus-pterygopalatine fossa-Meckel's cave approach. **Methods** Fifteen adult cadaver heads (30 sides) were dissected and the correlated anatomic landmarks were observed, measured and analyzed in an operative route. **Results** The approach was divided into 3 steps: entering the maxillary sinus, the later pterygopalatine fossa and the final Meckel's cave. Safe access to Meckel's cave could be achieved by tracing the vidian neurovascular bundles and dissecting the quadrangular space (QS). The distances from the nasal columella to the apertura maxillaries, the sphenopalatine foramen, and the anterior foramen of the pterygoid canal were (44.08±2.61) mm, (64.83±2.42) mm, and (70.43±2.94) mm, respectively. The angles between the horizontal plate of the palatine bone and the link from nasal columella to apertura maxillaries, between the horizontal plate of the palatine bone and the link from nasal columella to sphenopalatine foramen were (38.10±2.46)° and (26.15±2.26)°, respectively. **Conclusion** The endoscopic approach of transnasal maxillary sinus-pterygopalatine fossa-Meckel's cave (ENMPA) is a safe and direct way to access Meckel's cave, and could be employed for the treatment of tumor in Meckel's cave.

Keywords: endoscope; maxillary sinus; Meckel's cave; neuroanatomy

1 Introduction

Meckel's cave extends forward from the posterior fossa, and the ostium is located between the medial part of the petrous ridge below, the superior petrosal sinus above, and the lateral edge of the cavernous sinus medially[1]. The subarachnoid space extends forward within Meckel's cave to approximately the midportion of the gasserian ganglion. Disruption in Meckel's cave may lead to various abnormalities, among which trigeminal schwannomas (TS) and meningiomas are the most common[2-4]. Many surgical approaches to the lesions in Meckel's cave have been reported[5-7]. They are mainly divided into 3 groups, including anterolateral, lateral, and posterolateral approaches. However, none of these approaches can reach the entire Meckel's cave due to the difficulty in exposing the anteroinferomedial part of the cave[8]. With the development of nasal microsurgery, it is necessary to resect the tumors thoroughly, with less surgical damage to the adjacent structures. The endoscopic surgery to target the lesions in the pterygopalatine fossa and cavernous sinus have also been reported recently[9,10]. The anatomical structures involved in this approach are complicated, and the correlated anatomical research has been seldom reported[11]. In the present study, the nasal endoscopic approach to the target area was conducted, and the structures involved in this approach were observed and

Corresponding author: En-Yuan CAI
Tel & Fax: +86-0532-82912323
E-mail: cainoya@public.qd.sd.cn
Article ID: 1673-7067(2009)06-0376-07
CLC: R322.3+1
Document code: A
Received date: 2009-06-05

measured, in order to provide significant information for clinical application.

2 Materials and methods

2.1 Specimen Fifteen undamaged adult cadaver heads (30 sides), irrespective of gender, were provided by the Department of Anatomical Sciences, Qingdao University Medical College. The instruments used included a surgical microscope, microsurgery instruments, a headframe, a self-retaining retractor, Kirschner wires, a sliding caliper (accuracy 0.02 mm), a conimeter with pointer, and a DMC-FX8 Panasonic digital camera.

2.2 Methods and steps Through the nasal cavity-maxillary sinus-pterygopalatine fossa-Maeckl's cave (ENMPA) approach, the ipsilateral middle turbinate (20 sides), and the inferior turbinate (10 sides) were resected. By tracing the hiatus semilunaris inferior to the ethmoidal bulla, the horizontal uncinate process could be observed and then ectomized completely to obtain sufficient visual field. Then the ostium of the maxillary sinus was exposed (Fig. 1A). A wide nasomaxillary window was opened, enlarging the natural ostium of the maxillary sinus posteriorly, inferiorly, and superiorly. For better exposure and reconstruction of the cranial base after the surgery, the middle turbinate in the opposite nostril was removed or laterally displaced, and the sphenopalatine artery was dissected, exposing a nasoseptal pedicled flap on the posterior septal arteries of the contralateral side. After that, the posterior nasal septectomy was conducted[9]. The sphenopalatine foramen could be observed through tracing the nasal septum posterior branch of the sphenopalatine artery and the nasal posterolateral branch of the sphenopalatine artery, or by peeling the perpendicular plate periosteum of the palatine bone. The orbital process of the palatine was removed with back-biting rongeurs, in order to expose the fibroid tunica vaginalis that encased the sphenopalatine artery, the nasopalatine nerve and the posterolateral nasal rami of the maxillary nerve. The superior margin of the sphenopalatine foramen was enlarged and the sphenoidalis processus of the palatine bone was removed to expose the entire base of the pterygoid plates. After slightly pulling the tunica vaginalis surrounding the sphenopalatine artery, the pterygoid canal neurovascular bundle from the sphenopalatine ganglion in a posterosuperior to posteroinferior direction could be seen. The pharyngeal branch neurovascular bundle of the maxillary nerve, the greater palatine nerve and the lesser palatine nerve could also be observed. To provide a new safe approach to the pterygopalatine fossa and to observe the neurovascular relations, the posterior wall of the maxillary sinus was then removed in a superior direction up to the roof of the sinus, inferiorly to the floor of the sinus, medially to the vertical process of the palatine bone, and laterally to the angle between the lateral and posterior wall of the maxillary sinus. Adjacent structures were exposed (Fig. 1B).

The petrous segment of the internal carotid artery (ICA) and the maxillary nerve (V2) were identified by tracing the vidian neurovascular bundles, and then Meckel's cave was accessed. The foramen rotundum was ascertained by tracing V2, and the adjacent bone was drilled to expose the dura mater of the middle cranial fossa. The dura was then opened within a quadrangular space, with the ICA in the medial, the V2 in the lateral, and the horizontal petrous ICA in the inferior part. After that, the Meckel's cave and the petrous apex could be successfully accessed. To obtain an adequate operation area, the posterior ethmoid sinus and the wall of the sphenoid sinus were dissected. The adjacent structures were measured and analyzed. Field images were captured with the Panasonic DMC-FX8 DC camera. Measurement was conducted using a sliding caliper. Data were analyzed using the SPSS software and presented as mean±SD and 95% confidence interval.

3 Results

3.1 The nasal operational approach to Meckel's cave, using Kirschner wires, to observe the structures that needed dissection As shown in Fig. 2A, among the 30 sides, 60% (18 sides) needed removal of the middle turbinate, uncinate process, the anterior and lateral wall of the sphenoidal sinus, the medial wall of the maxillary sinus, and the posterior ethmoid cells; while 40% (12 sides) needed removal of the middle turbinate, inferior turbinate, uncinate process, the anterior and lateral wall of the sphenoidal sinus, the medial wall of the

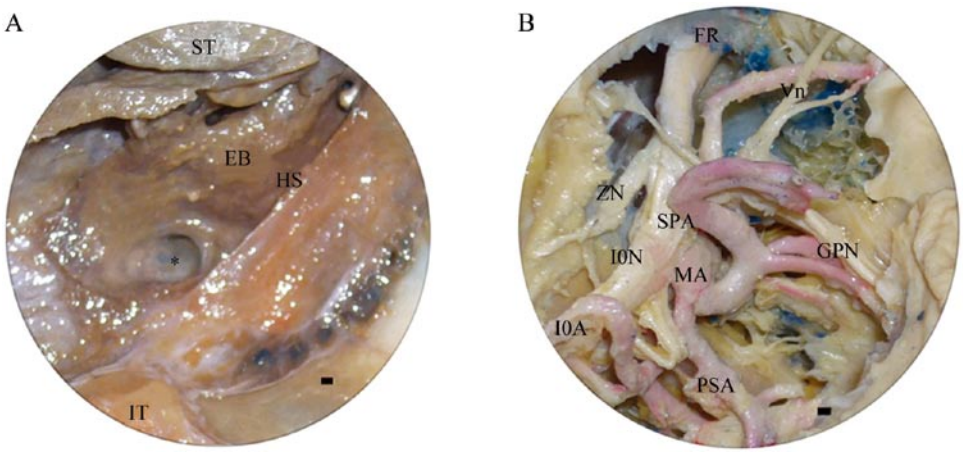

Fig. 1 **A: an endoscopy image which shows the ostium of the right maxillary sinus after removing the middle turbinate and uncinate process. B: an endoscopy image which shows the right pterygopalatine fossa. *: ostium of the maxillary sinus; EB: ethmoidal bulla; FR: foramen rotundum; GPN: greater palatine nerve; HS: hiatus semilunaris; IOA: infraorbital artery; ION: infraorbital nerve; IT: inferior turbinate; MA: maxillary artery; PSA: posterosuperior alveolar artery; SPA: sphenopalatine artery; ST: superior turbinate; vn: Vidian nerve; ZN: zygomatic nerve. Scale bar, 1 mm.**

Table 1. Measured distances and angles

	M (mm)		N (degrees)	
	Mean±SD	Range	Mean±SD	Range
The ostium of MS	44.08±2.61	43.11-45.06	38.10±2.46	37.18-39.01
Sphenopalatine foramen	64.83±2.42	63.93-65.74	26.15±2.26	25.30-26.99
Anterior foramen of pterygoid canal	70.43±2.94	69.33-71.53		
	-	-		

M: The distances from the nasal columella to the apertura maxillaries, to the sphenopalatine foramen, to the anterior foramen of the pterygoid canal; N: The included angles between the horizontal plate of the palatine bone and the line from the nasal columella to the apertura maxillaries, the line from the nasal columella to the sphenopalatine foramen; MS: maxillary sinus.

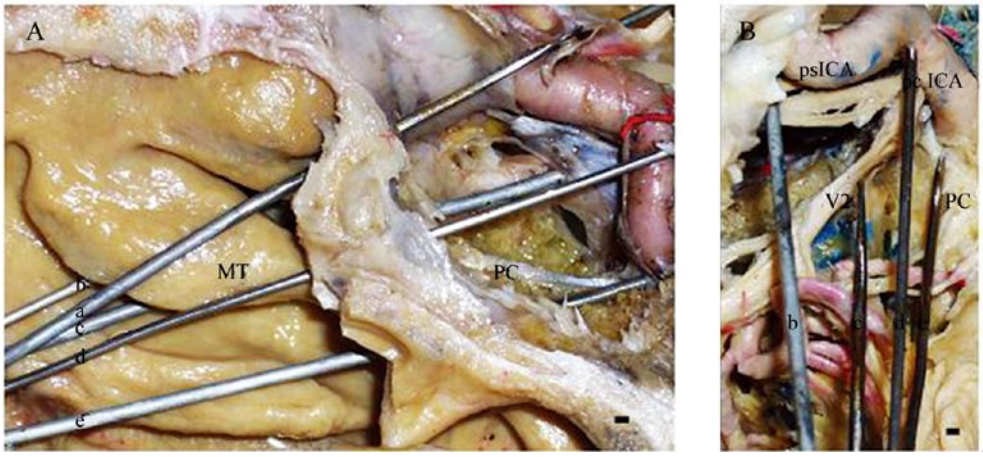

Fig. 2 **A: endonasal puncture to the right Meckel's cave using Kirschner wires. B: endonasal puncture to the right Meckel's cave using Kirschner wires after the obstacles were removed. a: the probe to sphenoidal ostium; b: the probe to superior orbital fissure; c: the probe to foramen rotundum; d: the probe to paraclival ICA; e: the probe to posterior foramen of pterygoid canal. MT: middle turbinate; PC: pterygoid canal; pcICA: paraclival ICA; psICA: parasellar ICA; V2: maxillary nerve. Scale bar, 1 mm.**

maxillary sinus and the posterior ethmoid cells.

3. 2 Measurement of the distances and angles The distances from the nasal columella to the apertura maxillaries, to the sphenopalatine foramen, and to the anterior foramen of pterygoid canal were measured, respectively. The included angles between the horizontal plate of the palatine bone and the line from nasal columella to the apertura maxillaries, and the line from nasal columella to the sphenopalatine foramen, were also measured, respectively. Data were shown in Table 1.

3.3 Analysis of correlated arteries using Kirschner wires to access the Meckel's cave As shown in Fig. 2B, after removing the obstacles, the sphenopalatine artery and vidian artery were shown to be involved in the approach to Meckel's cave. The diameter of sphenopalatine artery was (2.06±0.41) mm (ranging 1.91-2.21 mm), and the diameter of vidian artery was (1.10±0.33) mm (ranging 0.98-1.23 mm).

3.4 Segmentation of ICA via sphenoid sinus according to the report of Bouthillier[12] As shown in Fig. 3A, when the posterior wall of the sphenoidal sinus was exposed, the posterior paraclival ICA (pcICA) and the anterior parasellar ICA (psICA) were recognized based on their bony marks. The pcICA segment could be further subdivided into 2 parts: the posterior lacerum segment and the anterior trigeminal segment. The psICA segment could be subdivided into 4 parts in a posterior-to-anterior order: the posterior vertical segment, the inferior horizontal segment, the anterior vertical

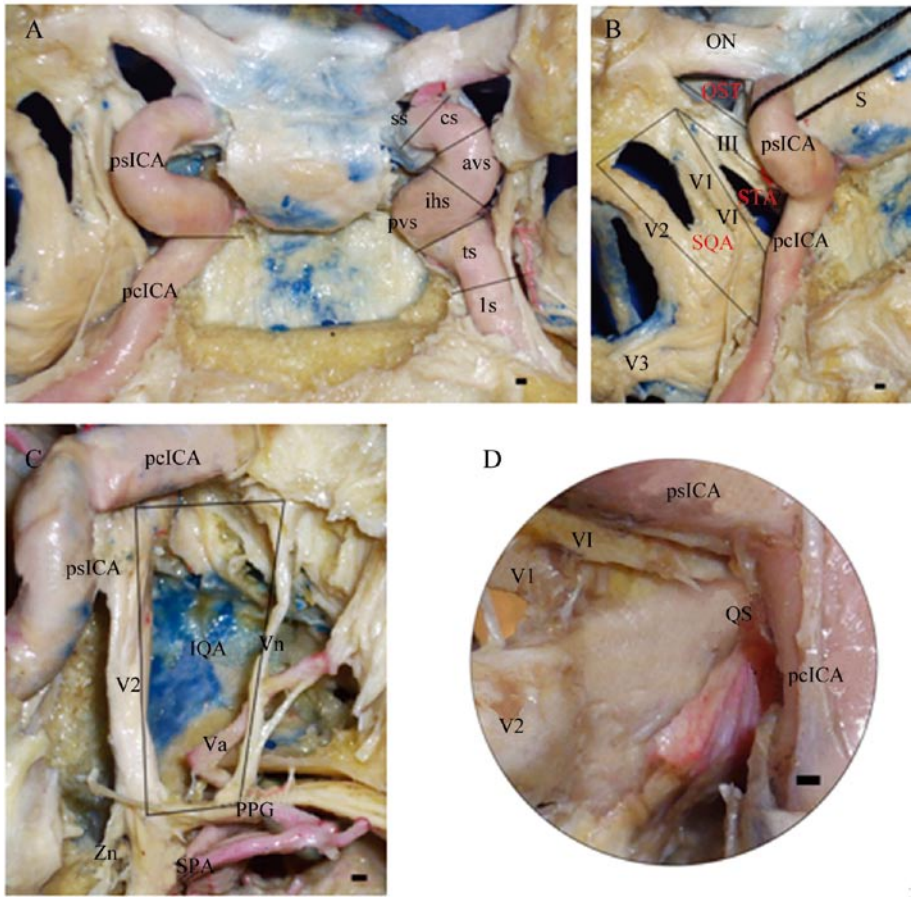

Fig. 3 A : ICA segment through sphenoid sinus. B and C: the relation of the right parasella neural and vascular structures through sphenoid sinus. D: a photograph of simulating endoscopy showing the right quadrangular space. avs: anterior vertical segment; cs: clinoidal segment; ihs: inferior horizontal segment; ls: lacerum segment; ON: optic nerve; PPG: pterygopalatine ganglion; pvs: posterior vertical segment; S: sella; SPA: sphenopalatine artery; ss: intracranial subarachnoid segment; ts: trigeminalsegment; va: vidian artery; V1: ophthalmic nerve; V2: maxillary nerve; V3: mandibular nerve; VI: abducens; vn: Vidian nerve; Zn: zygomatic nerve; III: oculomotor nerve. Scale bar, 1 mm.

segment, and the superior horizontal segment. The superior horizontal segment was composed of the clinoid segment of the ICA and the subarachnoid segment.

3. 5 Analysis of the parasellar neurovascular structures after removing the posterior wall of the sphenoidal sinus As shown in Fig. 3B and C, the parasellar neurovascular structures were divided as follows in the transsphenoidal approach: the optic strut triangle (OST), the superior triangular area (STA), the superior quadrangular area (SQA), and the inferior quadrangular area (IQA)(in a rostral-to-caudal order).

3.5.1 OST The lines of OST included the optic nerve above the optic strut of the anterior clinoid process, penetrating the optic foramen. The lateral was the oculomotor nerve which was below the optic strut and penetrated the superior orbital fissure (SOF). The basilar was the clinoid process segment of the ICA. The optic strut of the anterior clinoid was located in this triangle. When the sphenoid sinus was well pneumatized, OST represented the interoptic-carotid recess.

3.5.2 STA The superior part of STA was the oculomotor nerve, and the inferior part was the abducent nerve. The basilar part was the parasellar ICA. The surface of this area also consisted of the trochlear nerve and part of the ophthalmic nerve (V1).

3.5.3 SQA The top side of SQA was the abducent nerve and the inferior side was the maxillary nerve. The anterior base of SQA consisted of the bone of the lateral wall of the sphenoid sinus, which extended from SOF to the foramen rotundum. The posterior base was the trigeminal segment of ICA. V1 and the artery at the inferior part of cavernous sinus could be seen in this area.

3.5.4 IQA IQA could be seen when the sphenoid sinus was well pneumatized. The top part of IQA was V2, and the inferior part was the vidian nerve, which run from the lacerum segment of ICA to the pterygoid canal. Passing through this canal, it reached the pterygopalatine ganglion in the pterygopalatine fossa. The posterior side of IQA was the ICA lacerum segment. The anterior part was the sphenoid bone which linked the foramen rotundum to the pterygoid canal.

3.6 Observation of the quadrangular space (QS) Trace the vidian nerve through the pterygopalatine ganglion and remove the bottom and lateral wall of sphenoidal sinus. Meanwhile, V2 was also traced. Then, QS was exposed after the dura was opened, as shown in Fig. 3D.

The dura was opened within QS, which was bound by ICA medially, by V2 laterally, and by the horizontal petrous ICA inferiorly. QS was delimited by ICA at the medial and inferior positions, by V2 at the lateral side, and by the abducent nerve at the superior side. The abducent nerve ran upward obliquely and directly within the cavernous sinus, along the inferior margin of V1, into the superior orbital fissure. Via QS, the medial wall of Meckel's cave and petrous apex could be accessed. The lateral wall of Meckel's cave could also be achieved via the V1-V2 triangle and the V2-V3 triangle.

Table 2. Length of the sides of OST and STA (mm)

	the medial side		the lateral side		the base	
	Mean±SD	Range	Mean±SD	Range	Mean±SD	Range
OST	5.16±0.83	4.85-5.47	6.15±1.15	5.72-6.58	4.93±1.07	5.53-5.33
STA	9.45±2.13	8.66-10.24	11.98±2.71	10.97-13.00	8.82±2.91	7.73-9.91

Table 3. Length of the sides of SQA and IQA (mm)

		the medial side	the lateral side	the anterior base	the posterior base
SQA	Mean±SD	11.98±2.71	14.79±1.97	7.22±1.60	6.00±1.42
	Range	10.97-13.00	14.06-15.53	6.62-7.81	5.47-6.53
IQA	Mean±SD	14.79±1.97	17.74±1.56	6.11±1.41	7.80±1.23
	Range	14.06-15.53	17.16-18.32	5.58-6.63	7.34-8.25

3.7 The lengthen of the parasellar triangle sides The lengthen of the parasella triangle sides was shown in Table 2 and Table 3.

4 Discussion

Meckel's cave is adjacent to the caverous sinus. It is surrounded by complicated structures. Smith RW was the first to investigate a primary tumor of the gasserian ganglion in 1836[13]. To date, 3 primary approaches, including the anterolateral, the lateral, and the posterior lateral approaches, have been used to access this central region[8].

The anterolateral approach relies on the pterion region as an entry point to access Meckel's cave[5,14-17]. To reach the anterior part of the medial component of Meckel's cave, the anteromedial and the anterolateral triangles of the middle cranial fossa need to be traversed[15,17,18]. This approach is applied mainly to remove the intracranial trigeminal schwannomas (TS) predominantly located in the middle fossa. However, it still has some defects, such as the need for temporal lobe crushing, the damage to the sphenoparietal, the sphenobasal and the sphenopetrosal Sinuses, and the transgression of the trigeminal nerve which may lead to nervous dysfunction.

The lateral approach, such as the extended middle fossa approach, Kawase's approach, a combined temporal craniotomy-presigmoidal method and the temporal base transtentorial approach, is mainly applied to intracranial dumbbell-shaped TS in the middle and the posterior fossa. This approach be classified into extradural and intradural groups. The disadvantages include the need of temporal lobe retraction, the damage to the vein of Labbé, the superior petrosal sinus and the temporobasal veins, and the risk of injuries to critical structures of the petrous bone that guards the Meckel's cave, such as the middle ear structures, the facial nerve, and the petrous segment of ICA[19].

The posterolateral approach is the modification of the standard retrosigmoid approach, in that the suprameatal drilling is added to allow access to Meckel's cave[6,7]. This approach is mainly applied to intracranial TS in the posterior fossa. However, in a retrosigmoid route, it is necessary to carefully treat all the cranial nerves that are superficial or dorsal to the lesion.

At present, various approaches (anterolateral, lateral, and posterior lateral approaches) to treat the lesions in Meckel's cave all had the difficulty to expose the anteroinferomedial aspect of the cave. The trigeminal nerve needs to be manipulated, since it guards the anteromedial compartment of Meckel's cave[6]. For intracranial TS predominantly located in the cerebellopontine angle, particularly in patients with normal trigeminal function, the ENMPA is not a suitable choice. The standard lateral and posterior approaches are better. As a result, the location and the size of the lesion in Meckel's cave are the major factor in deciding approaches for surgical treatment.

The ENMPA approach provides a direct route to the anteromedial region of Meckel's cave, which may be helpful for the dissection between the trigeminal nerve and the periosteal layer of the dura mater for lesions within the inferomedial part of Meckel's cave.

To study this approach, we dissected and measured the related structures. Furthermore, we measured and analyzed cavernous sinus and Vidian nerve through sphenoid sinus. The present study on ENMPA may offer new hints for the treatment of various tumors within Meckel's cave.

Acknowledgement: This work was supported by the National key Technology R & D Program during the Eleventh Five-Year Plan Period of China (No. 2006BAI01A12).

References:

[1] Rhoton AL Jr. The cavernous sinus, the cavernous venous plexus, and the carotid collar. Neurosurgery 2002, 51: S375-410.

[2] Kouyialis AT, Stranjalis G, Papadogiorgakis N, Papavlassopoulos F, Ziaka DS, Petsinis V, *et al*. Giant dumbbell-shaped middle cranial fossa trigeminal schwannoma with extension to the infratemporal and posterior fossae. Acta Neurochir (Wien) 2007, 149: 959-964.

[3] Verstappen CC, Beems T, Erasmus CE, van Lindert EJ. Dumbbell trigeminal schwannoma in a child: Complete removal by a one-stage pterional surgical approach. Childs Nerv Syst 2005, 21: 1008-1011.

[4] Zhu JJ, Padillo O, Duff J, Hsi BL, Fletcher JA, Querfurth H.

Cavernous sinus and leptomeningeal metastases arising from a squamous cell carcinoma of the face: Case report. Neurosurgery 2004, 54: 492-499.

[5] Inoue T, Rhoton AL Jr, Theele D, Barry ME. Surgical approaches to the cavernous sinus: A microsurgical study. Neurosurgery 1990, 26: 903-932.

[6] Samii M, Tatagiba M, Carvalho GA. Retrosigmoid intradural suprameatal approach to Meckel's cave and the middle fossa: Surgical technique and outcome. J Neurosurg 2000, 92: 235-241.

[7] Samii M, Carvalho GA, Tatagiba M, Matthies C. Surgical management of meningiomas originating in Meckel's cave. Neurosurgery 1997, 41: 767-775.

[8] Kassam AB, Prevedello DM, Carrau RL, Snyderman CH, Gardner P, Osawa S, *et al*. The front door to meckel's cave: an anteromedial corridor via expanded endoscopic endonasal approach- technical considerations and clinical series. Neurosurgery 2009, 64: 71-83.

[9] Wormald PJ, Van Hasselt A. Endoscopic removal of juvenile angiofibromas. Otolaryngol Head Neck Surg 2003, 129(6): 684-691.

[10] Cavallo LM, Dal Fabbro M, Jalalod'din H, Messina A, Esposito I, Esposito F, *et al*. Endoscopic endonasal transsphenoidal surgery. Before scrubbing in: tips and tricks. Surg Neurol 2007, 67: 342-347.

[11] Huang XC, Xu W, Jiang JY. Effect of resuscitation after selective cerebral ultraprofound hypothermia on expressions of nerve growth factor and glial cell line-derived neurotrophic factor in the brain of monkey. Neurosci Bull 2008, 24(3): 150-154.

[12] Bouthillier A, van Loveren HR, Keller JT. Segments of the internal carotid artery: a new classification. Neurosurgery 1996, 38: 425-433.

[13] Moiyadi AV, Satish S, Rao G, Santosh V. Multicompartmental trigeminal schwannoma--a clinical report. J Craniofac Surg 2008, 19: 1177-1180.

[14] Jian FZ, Santoro A, Innocenzi G, Wang XW, Liu SS, Cantore G. Frontotemporal orbitozygomatic craniotomy to exposure the cavernous sinus and its surrounding regions. Microsurgical anatomy. J Neurosurg Sci 2001, 45(1): 19-28.

[15] Krisht AF. Transcavernous approach to diseases of the anterior upper third of the posterior fossa. Neurosurg Focus 2005, 19(2): E2.

[16] Taha JM, Tew JM Jr, van Loveren HR, Keller JT, el-Kalliny M. Comparison of conventional and skull base surgical approaches for the excision of trigeminal neurinomas. J Neurosurg 1995, 82: 719-725.

[17] Yasuda A, Campero A, Martins C, Rhoton AL Jr, de Oliveira E, Ribas GC. Microsurgical anatomy and approaches to the cavernous sinus. Neurosurgery 2008, 62: 1240-1263.

[18] Yasuda A, Campero A, Martins C, Rhoton AL Jr, Ribas GC. The medial wall of the cavernous sinus: Microsurgical anatomy. Neurosurgery 2004, 55: 179-190.

[19] Sanna M, Bacciu A, Pasanisi E, Taibah A, Piazza P. Posterior petrous face meningiomas: An algorithm for surgical management. Otol Neurotol 2007, 28: 942-950.

模拟内镜下经鼻 - 翼腭窝至 Meckel 腔入路的应用解剖学研究

白志强[1]，蔡恩源[1]，王时强[1]，李照建[1]，王守彪[2]

[1] 青岛大学医学院附属医院神经外科一病区， 青岛 266003

[2] 青岛大学医学院解剖学教研室，青岛 266071

摘要：目的 通过对鼻腔 - 上颌窦 - 翼腭窝 -Meckel 腔入路的内镜解剖学研究，为治疗 Meckel 腔肿瘤提供新的入路选择。**方法** 对 15 具动静脉灌注乳胶的成人尸头标本进行模拟鼻内镜下该入路分层显微解剖，对相关解剖标志进行了观察、分析、拍摄和测量。**结果** 该入路分为三步：进入上颌窦，进入翼腭窝，最后进入 Meckel 腔。追踪翼管神经血管束，解剖分离四方形空间可安全到达 Meckel 腔。鼻小柱至上颌窦口、蝶腭孔、翼管前孔距离分别为(44.08±2.61) mm、(64.83±2.42) mm 和(70.43±2.94) mm。鼻小柱至上颌窦口连线，及其至蝶腭孔连线与腭骨水平板的夹角分别为 (38.10±2.46)°和 (6.15±2.26)°。**结论** 鼻内镜下鼻腔-上颌窦-翼腭窝-Meckel腔入路是到达Meckel腔前下内面的安全且直接的入路，可用来治疗 Meckel 腔肿瘤。

关键词：内镜；上颌窦；Meckel 腔；神经解剖